科学通报 2017 年 第 62 卷 第 35 期: 4123 ~ 4130
专题: 新概念有机发光材料 论 文
《中国科学》杂志社
SCIENCE CHINA PRESS

咪唑取代的三苯甲基自由基的合成表征及其光学性质

艾心, 李峰*

吉林大学化学学院, 超分子结构与材料国家重点实验室, 长春 130012
* 联系人, E-mail: lifeng01@jlu.edu.cn

2017-08-21 收稿, 2017-09-13 修回, 2017-09-21 接受, 2017-10-31 网络版发表
国家重点研发计划(2016YFB0401001)和国家自然科学基金(51673080)资助

摘要 有机发光自由基材料是一类新型的发光材料, 从分子轨道的电子排布来看, 其发光是区别于传统材料的双线态激子发光. 目前具有发光性质的有机自由基材料种类较少, 并且大部分分子稳定性差、荧光量子产率低. 本文以稳定性较差、荧光量子产率较低的三(2,4,6-三氯代苯基)甲基自由基(TTM)为骨架, 在分子外围引入咪唑基团, 得到两种改良的发光自由基TTM-Imz2和TTM-Imz3, 详细表征了两者的光物理性质和稳定性, 并应用于有机电致发光器件(OLEDs). 结果表明, 两者溶液中的荧光量子产率及稳定性相比于TTM均有大幅提升, 并实现了波长较短的橙光发射, 其中以TTM-Imz3制备的橙光OLED的最大外量子效率达到2.9%.

关键词 有机发光自由基, 双线态, 咪唑, 橙光发射, 荧光量子产率, 稳定性, 有机电致发光器件

有机发光材料在材料科学领域有着广泛的应用, 例如用于电致发光器件(OLEDs)[1,2]以及化学传感器[3]. 传统的有机发光材料辐射跃迁产生光子, 从原理上来讲, 主要分为荧光和磷光两类. 两者的主要区别在于发光材料分子激发态外层的2个未成对电子的自旋方向是平行还是反平行的. 近年来, 有机发光自由基材料作为一类新型的发光材料开始引起人们的关注[4~9]. 与传统的发光材料不同, 自由基发光材料分子轨道最外层只有1个电子[10,11], 是双线态激子发光. 因此, 将其应用于电致发光器件时, 可以避开电激发条件下传统有机发光材料三线态激子的利用问题, 通过双线态激子发光, 实现接近100%的可用于发光的双线态激子的生成比例, 从而提高器件效率[11,12].

本研究组[11]首次阐述了将自由基材料作为发光层的意义, 并使用一种稳定的深红光自由基材料作为发光层制备OLED, 原型器件最大外量子效率(EQE)达到2.4%. 对器件结构进一步优化后, 最大EQE达到4.3%, 同时也证实了接近100%的双线态激子的生成比例[12]. 自由基通常情况下是不稳定的, 具有很高的反应活性, 因此大部分自由基的光谱性质都是在瞬态条件下测试得到的[13]. 既便是稳定的自由基, 能够在室温条件下产生荧光发射的种类也非常少[4,5,8,9,14,15], 部分分子只有在77 K甚至更低温度条件下才能检测到微弱的荧光发射, 同时, 稳定自由基分子发光光色大部分集中在红光范围内[16~18]. 此外, 当分子中既有荧光基团又存在自由基时, 有些自由基会淬灭分子内荧光团的荧光, 使整个分子不发光[19,20]; 也有些自由基不能有效地淬灭荧光团的荧光, 使分子还带有荧光团的荧光性质, 但自由基部分也没有对发光产生贡献[21]. 其次, 稳定的发光自由基在室温条件下, 也会面临因发生化学反应而降解的问题[22,23]. 因此, 通过合理的分子设计、引入特定的基团来合成具有发光性质的新自由基分子, 并提高分子的稳定性、荧光量子产率以及调节自由基发光的光色, 是开发新型发光自由基材料的主要方向.

引用格式: 艾心, 李峰. 咪唑取代的三苯甲基自由基的合成表征及其光学性质. 科学通报, 2017, 62: 4123–4130
Ai X, Li F. Synthesis and characterization of imidazole substituted trityl radicals and its optical properties (in Chinese). Chin Sci Bull, 2017, 62: 4123–4130, doi: 10.1360/N972017-00896

© 2017《中国科学》杂志社

本文以三(2,4,6-三氯代苯基)甲基自由基(TTM)为骨架, 通过在外围引入含氮五元杂环咪唑, 扩大分子的共轭体系, 调节整个分子的性质, 得到了TTM-Imz2, TTM-Imz3两种新型稳定发光自由基. 通过气质联用仪(GC-MS), 傅里叶变换红外光谱仪(FT-IR)、电子顺磁共振谱仪来对自由基进行表征. 随后, 通过紫外可见光谱(UV-vis)、稳态/瞬态荧光光谱、热失重分析、理论计算等方法对自由基分子的光物理性质及稳定性进行了系统研究. 最终, 将自由基分子应用于电致发光器件中, 并对其器件性能进行表征.

1 实验

(ⅰ) 试剂与仪器. 超干四氢呋喃购于安耐吉公司, 液体试剂购于北京化工厂, 其余化学药品购于百灵威公司. TTM采用文献[24,25]报道的方法制备. GC-MS通过Thermo Fisher公司的ITQ1100离子阱型气相色谱-质谱联用仪测试; FT-IR通过Brucker公司的VERTEX 80V傅里叶变换红外光谱仪测试; 电子顺磁共振通过日本电子JES-FA200电子自旋共振谱仪测试; 紫外可见光谱通过日本岛津公司UV-2250紫外可见分光光度计测试; 荧光光谱通过日本岛津5301PC荧光光谱仪测试; 瞬态荧光光谱通过爱丁堡公司FLS980稳态/瞬态荧光光谱仪测试; 测量溶液中的荧光量子产率时, 使用罗丹明6G的乙醇溶液(φ=0.95)作为参比, 激发光波长380 nm; 密度泛函计算(DFT)使用Guassian09程序、B3LYP泛函、6-31G(d,p)基组计算得到; 热重分析(TGA)通过美国TA公司Q500热失重分析仪测试; 光稳定性测试所用脉冲激光波长为350 nm, 功率密度为318.4 kW/cm^2, 脉冲宽度为8 ns, 频率为10 Hz; OLED器件在2×10^{-4} Pa下采用真空热蒸镀法制备, 其电流密度-电压特性通过Keithley 2400测试, 亮度-电压特性以及电致发光光谱通过PR650测试.

(ⅱ) 化合物HTTM-Imz2和HTTM-Imz3的合成. 在100 mL圆底烧瓶中加入TTM(1.0 g, 1.8 mmol)、咪唑(0.62 g, 9.1 mmol)、碳酸铯(0.94 g, 2.6 mmol)以及*N*,*N*-二甲基甲酰胺20 mL, 氮气保护下, 160℃避光反应5 h. 随后冷却至室温, 加入200 mL去离子水后抽滤得粗产物. 对粗产物使用柱层析色谱进一步提纯(洗脱剂为乙酸乙酯), 得到红色固体粉末HTTM-Imz2和HTTM-Imz3. HTTM-Imz2, 0.20 g, 产率18%, GC-MS 615.66; HTTM-Imz3, 800 mg, 产率69%, GC-MS 647.78.

(ⅲ) 化合物TTM-Imz2和TTM-Imz3的合成. 在100 mL圆底烧瓶中加入HTTM-Imz2(0.18 g, 0.29 mmol)、叔丁醇钾(0.072 g, 0.64 mmol)以及50 mL超干四氢呋喃. 氮气保护下, 避光搅拌1.5 h, 然后加入四氯苯醌(TCQ, 0.21 g, 0.85 mmol), 继续搅拌1 h. 避光条件下, 将溶剂旋干得到粗产物, 再通过柱层析进一步提纯(洗脱剂为乙酸乙酯)后得到红色固体粉末TTM-Imz2. TTM-Imz2, 0.15 g, 产率83%, GC-MS 614.96, FT-IR(KBr, cm^{-1}) 3113(w), 2957(w), 2928(w), 2870(w), 2854(w), 1722(w), 1585(s), 1560(m), 1545(s), 1493(s), 1406(w), 1373(w), 1306(s), 1261(w), 1248(w), 1196(w), 1184(w), 1138(w), 1122(w), 1107(w), 1059(m), 997(w), 900(w), 858(w), 806(s), 725(w), 654(w), 600(w), 563(w), 436(w). TTM-Imz3的合成方法同上. TTM-Imz3, 产率85%, GC-MS 647.02, FT-IR(KBr, cm^{-1}) 3123(w), 3111(w), 3074(w), 3043(w), 2961(w), 2928(w), 1726(w), 1585(s), 1543(s), 1493(s), 1406(m), 1304(s), 1261(s), 1120(m), 1107(m), 1061(s), 997(m), 902(w), 866(m), 827(w), 802(s), 768(w), 739(m), 704(w), 656(s), 627(w), 606(w), 590(w), 432(w). TTM-Imz2和TTM-Imz3的合成路线如图1所示.

2 结果与讨论

2.1 电子顺磁共振

为了验证合成的自由基中单电子的存在, 分别对TTM-Imz2和TTM-Imz3两种自由基分子的固体样品进行了室温电子顺磁共振测试(EPR), 结果如图2所示. 两种样品的EPR谱均有明显信号, $g_{\text{TTM-Imz}_2}$=2.0040, $g_{\text{TTM-Imz}_3}$=2.0038, 与理想情况下的自由电子的g值(g=2.0023)非常接近, 证实了样品中单电子的存在.

2.2 光物理性质

TTM-Imz2和TTM-Imz3在二氯甲烷溶液中的紫外可见吸收光谱如图3(a)所示. 与其他三苯甲基类自由基[26]相似, 两种自由基均在短波长和长波长区有一强一弱2个特征吸收带. 其中TTM-Imz2的吸收峰波长为382和552 nm, TTM-Imz3的吸收峰波长为390和558 nm, 与TTM-Imz2相比有轻微红移.

图3(b)和(c)为两种自由基分子在不同溶剂中的荧光光谱. 从图中可以看出, 两种自由基在不同溶剂

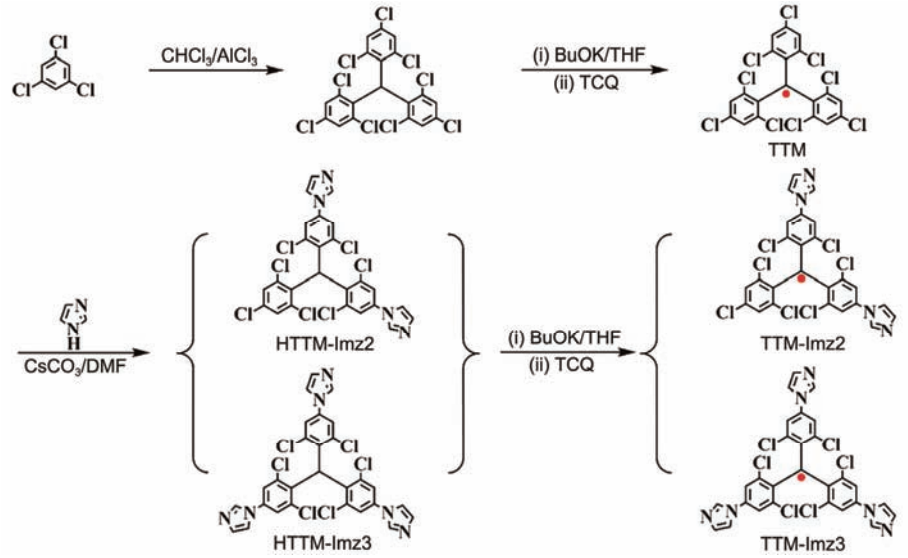


图 1 (网络版彩色)TTM-Imz2 和TTM-Imz3 的合成路线
Figure 1 (Color online) Synthetic routes for TTM-Imz2 and TTM-Imz3

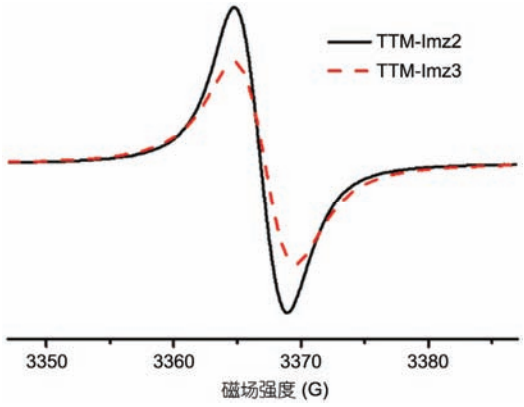


图 2 (网络版彩色)TTM-Imz2 和TTM-Imz3 固体的室温EPR谱
Figure 2 (Color online) Solid EPR spectra of TTM-Imz2 and TTM-Imz3 at room temperature

中的荧光光谱的峰形基本保持不变，峰位置与TTM自由基[26]相比红移20 nm左右，均呈现橙光发射. 在正己烷溶剂中TTM-Imz2光谱的峰位置为581 nm, TTM-imz3为584 nm. 随着溶剂极性的变化，两者光谱的峰位置并没有明显的变化(TTM-Imz2峰位置从581 nm变化到589 nm, TTM-Imz3峰位置从584 nm变化到590 nm)，说明两种自由基的发光具有非常弱的电荷转移(CT)态性质. 以罗丹明6G的乙醇溶液为参比，在氯仿溶液中测得TTM-Imz2的荧光量子产率为5.9%，TTM-Imz3为10.5%，相比于TTM(φ=0.15%)[26]分别提高了约39和70倍. 通过瞬态荧光衰减测试得到在氯仿溶液中TTM-Imz2的激发态寿命为12.8 ns, TTM-Imz3为16.1 ns，均位于传统的荧光发射的激发态寿命范围内. 因此，咪唑基团的引入，在大幅提升TTM自由基荧光量子产率的同时，荧光光谱峰位置只红移了20 nm左右，得到了区别于红光的橙光发射.

2.3 理论计算

为了进一步分析两种自由基分子的分子轨道、电子云分布以及咪唑基团的影响，我们借助高斯09程序，通过DFT计算对两种自由基分子的基态结构进行优化. 图4(a)和(b)为两种自由基分子优化后的基态结构，从中可以发现TTM-Imz2和TTM-Imz3的中心碳原子为sp^2杂化，与相邻的3个碳原子形成平面结构，咪唑部分与邻近的TTM骨架上苯环的夹角均为33°~35°. 随后，我们进一步分析两种分子的前线轨道(图4(c)和(d))，TTM-Imz2和TTM-Imz3的单电子占据轨道(SOMO)分别为155α和164α，能量相近且电子云主要集中在中心碳原子上，同时也部分扩展到邻近的苯环及引入的咪唑单元上. 因此，咪唑基团的引入，与整个分子形成了的一定程度的共轭，减小了SOMO与最低未占据轨道之间的能量差(TTM为2.31 eV[5], TTM-Imz2为2.22 eV, TTM-Imz3为2.19 eV)，导致了光谱相对于TTM的红移.

2.4 稳定性

为了评价两种自由基分子的稳定性，我们首先对其进行了热失重分析(TGA)测试，结果如图5(a)所

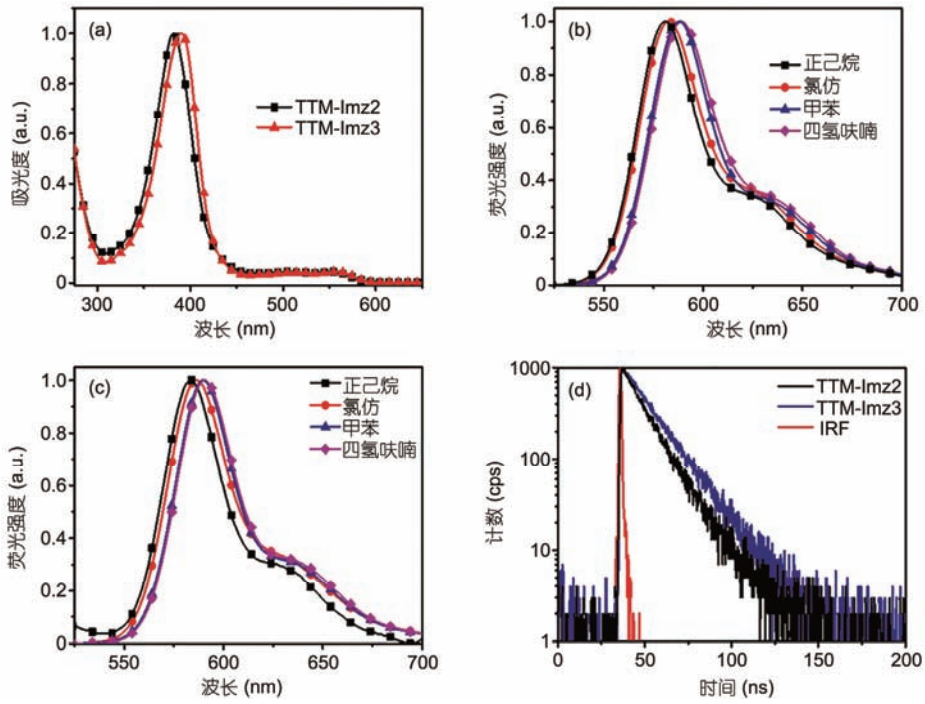


图 3 (网络版彩色)光物理性质. (a) TTM-Imz2 和TTM-Imz3 在二氯甲烷中的紫外可见吸收光谱; TTM-Imz2(b)和TTM-Imz3(c)在不同溶剂中的荧光光谱; (d) TTM-Imz2 和TTM-Imz3 在氯仿溶液的瞬态荧光(PL)衰减

Figure 3 (Color online) Photophysical properties. (a) Absorption spectra of TTM-Imz2 and TTM-Imz3 in CH_2Cl_2. Emission spectra of TTM-Imz2 (b) and TTM-Imz3 (c) in various solvents. (d) Transient PL decay of TTM-Imz2 and TTM-Imz3 in $CHCl_3$

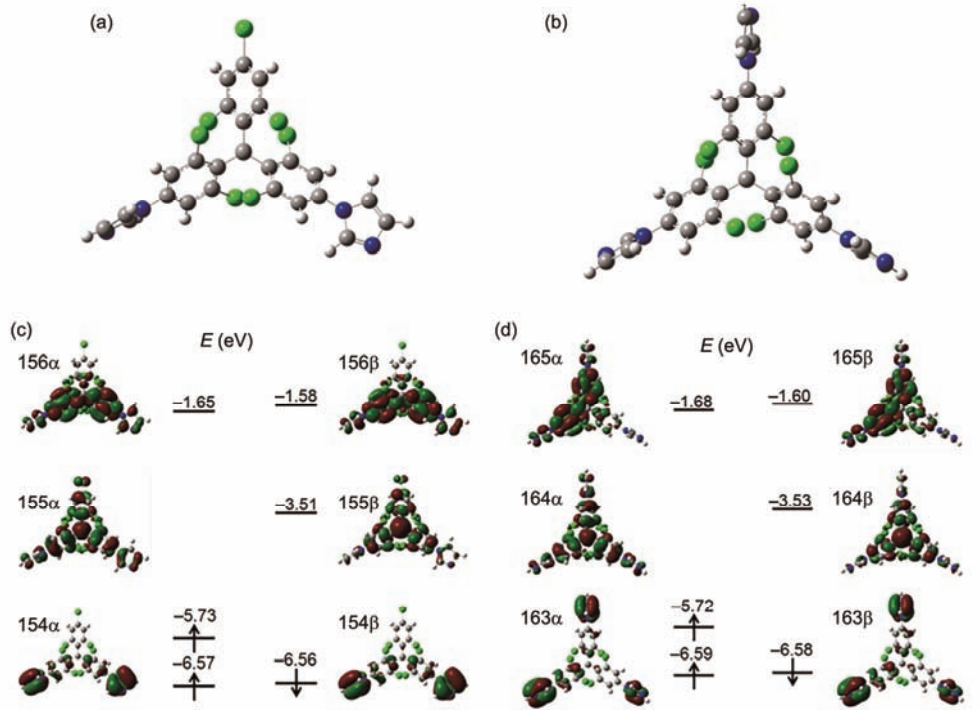


图 4 (网络版彩色)DFT计算优化得到的TTM-Imz2(a)和TTM-Imz3(b)的基态结构; TTM-Imz2(c)和TTM-Imz3(d)分子的前线轨道

Figure 4 (Color online) Optimized ground state structure of TTM-Imz2 (a) and TTM-Imz3 (b) through DFT calculations. Frontier orbitals of TTM-Imz2 (c) and TTM-Imz3 (d)

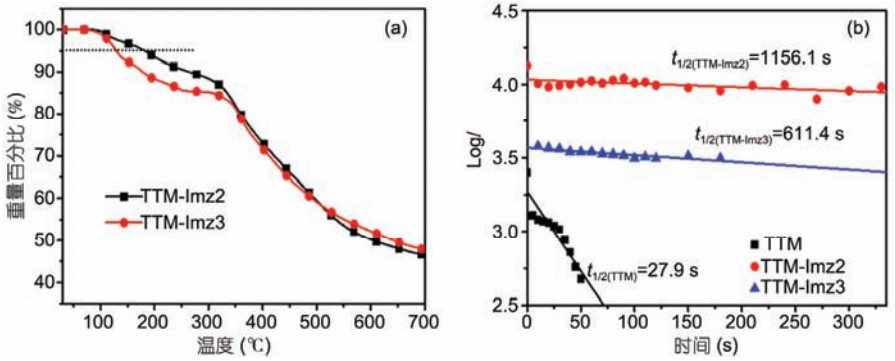


图 5 (网络版彩色)稳定性测试结果. (a) TTM-Imz2 和TTM-Imz3 的热重分析测试; (b) 在 350 nm脉冲激光照射下, TTM, TTM-Imz2, TTM-Imz3 的甲苯溶液的荧光强度的衰减

Figure 5 (Color online) The results of stability test. (a) TGA measurements of TTM-Imz2 and TTM-Imz3. (b) PL decay of TTM, TTM-Imz2 and TTM-Imz3 in toluene under excitation of a pulse laser with λ_{ex}=350 nm

示. 相比之下, TTM-Imz2较为稳定, 在其重量损失5%时的热分解温度为182℃; TTM-Imz3的热稳定性稍差, 其重量损失5%时的热分解温度仅为129℃. 随后, 使用波长为355 nm的脉冲激光对两种自由基的氯仿溶液照射, 记录光强随时间的变化, 并在相同条件下测试TTM作为对比. 从图5(b)中可以看出, TTM的光稳定性很差, 在脉冲激光(波长为355 nm, 功率密度为318.4 kW/cm^2, 脉冲宽度为8 ns, 频率为10 Hz)的照射下荧光强度迅速降低, 半衰期仅有27.9 s; 而引入咪唑基团后, 自由基的稳定性有较大幅度的提升, 荧光强度缓慢降低, 半衰期分别达到1156.1 s (TTM-Imz2)和611.4 s (TTM-Imz3), 是TTM的41.4和21.9倍.

2.5 电致发光性质

我们将两种自由基应用于OLEDs中来研究其电致发光性质. TTM-Imz2和TTM-Imz3固体粉末均存在较强的聚集淬灭现象, 因此采用主客体掺杂的方式, 将自由基材料掺杂于TPBi中, 同时使用TAPC作为空穴传输层、PO-T2T作为电子传输层, 通过真空热蒸镀法制备掺杂器件, 其优化后的器件结构如图6(a)所

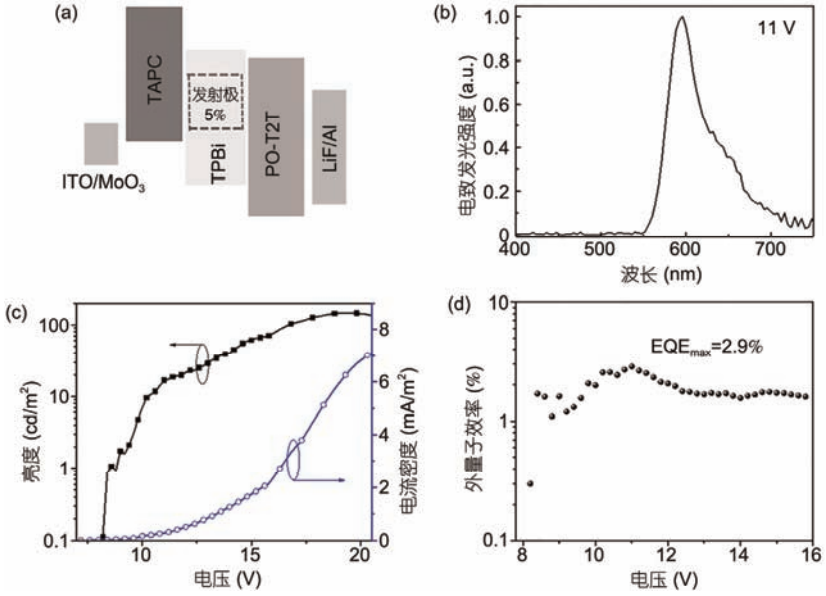


图 6 (网络版彩色)器件结构及性能. (a) TTM-Imz2 和TTM-Imz3 的电致发光器件结构; (b) TTM-Imz3 器件在 11 V的电致发光光谱; (c) TTM-Imz3 器件的亮度和电流密度随电压的变化; (d) TTM-Imz3 器件的EQE随电压的变化

Figure 6 (Color online) Devices structure and performance. (a) Structure of TTM-Imz2 and TTM-Imz3 based OLEDs. (b) EL spectra of TTM-Imz3 based OLEDs at 11 V. (c) The *J-V-L* characteristics of TTM-Imz3 based OLEDs. (d) The EQE of TTM-Imz3 based OLEDs as a function of voltage

表 1 TTM-Imz2 和TTM-Imz3 的电致发光性能数据[a)]
Table 1 OLED properties of TTM-Imz2 and TTM-Imz3

器件	V_{on}(V)	L(cd/m^2)	EQE(%)	λ_{EL}(nm)
TTM-Imz2	7.6	14	1.1	588
TTM-Imz3	8.6	147	2.9	592

a) V_{on}, 亮度为1 cd/m^{2}时的开启电压; L, 器件最大亮度; EQE, 最大外量子效率; λ_{EL}, 电致发光波长

示(ITO/MoO_3(3 nm)/TAPC(70 nm)/TTM-Imz2或TTM-Imz3∶TPBi(5%, 质量百分比, 40 nm)/PO-T2T(70 nm)/LiF(0.8 nm)/Al(100 nm)). 两者的器件性能数据总结于表1中. 从表1中可以看出, 基于TTM-Imz2和TTM-Imz3的OLED的发光光谱峰位置相比于溶液中有轻微的红移, 分别为588和592 nm. 以电致发光性能更优的TTM-Imz3器件为例, 其电致发光光谱在10~20 V非常稳定(图S1(a)), 与溶液中测得的谱图形状相同, 且在可见光范围内没有其他发光物质的干扰; 其亮度-电压-电流密度(*J*-*V*-*L*)图如图6(c)所示(电流效率-电流密度图见图S1(b)). TTM-Imz3器件的最大亮度达到147 cd/m^2, 外量子效率在电压为11 V时达到最大值2.9%.

3 结论

本文通过在稳定性较差、荧光量子产率较低的发光自由基TTM骨架上引入不同数量的咪唑基团, 得到了两种改良的发光自由基TTM-Imz2和TTM-Imz3, 并详细地表征了两者的光物理性质和稳定性. 两种材料均呈现橙光发射, 在发射波长没有大幅度红移的情况下, 大幅改善了TTM的荧光量子产率及稳定性. 其中, 以参比法测得的TTM-Imz2和TTM-Imz3在氯仿溶液中的荧光量子产率分别达到5.9%和10.5%, 相比TTM分别提高了约39和70倍. 热失重分析表明, TTM-Imz2有着相对较高的热分解温度, 达到182℃. 在紫外脉冲激光照射下, 两种自由基均表现出较高的光稳定性, 其半衰期分别达到TTM的41.4倍(TTM-Imz2)和21.9倍(TTM-Imz3). 使用两种自由基制备的OLED均实现波长较短的橙光发射, 其中TTM-Imz3器件最大亮度达到147 cd/m^2, 最大外量子效率达到2.9%.

参考文献

1 Tang C W, VanSlyke S A. Organic electroluminescent diodes. Appl Phys Lett, 1987, 51: 913–915
2 Ma Y, Zhang H, Shen J, et al. Electroluminescence from triplet metal-ligand charge-transfer excited state of transition metal complexes. Synth Met, 1998, 94: 245–248
3 Callan J F, de Silva A P, Magri D C. Luminescent sensors and switches in the early 21st century. Tetrahedron, 2005, 61: 8551–8588
4 Velasco D, Castellanos S, López M, et al. Red organic light-emitting radical adducts of carbazole and tris(2,4,6-trichlorotriphenyl)methyl radical that exhibit high thermal stability and electrochemical amphotericity. J Org Chem, 2007, 72: 7523–7532
5 Hattori Y, Kusamoto T, Nishihara H. Luminescence, stability, and proton response of an open-shell (3,5-dichloro-4-pyridyl)bis(2,4,6-trichlorophenyl)methyl radical. Angew Chem Int Ed, 2014, 53: 11845–11848
6 Hattori Y, Kusamoto T, Nishihara H. Enhanced luminescent properties of an open-shell (3,5-dichloro-4-pyridyl)bis(2,4,6-trichlorophenyl)methyl radical by coordination to gold. Angew Chem Int Ed, 2015, 54: 3731–3734
7 Heckmann A, Lambert C. Neutral organic mixed-valence compounds: Synthesis and all-optical evaluation of electron-transfer parameters. J Am Chem Soc, 2007, 129: 5515–5527
8 Lannes A, Intissar M, Suffren Y, et al. Terbium (iii) and yttrium (iii) complexes with pyridine-substituted nitronyl nitroxide radical and different beta-diketonate ligands. Crystal structures and magnetic and luminescence properties. Inorg Chem, 2014, 53: 9548–9560
9 Tretyakov E V, Plyusnin V F, Suvorova A O, et al. Luminescence of the nitronyl nitroxide radical group in a spin-labelled pyrazolylquinoline. J Lumin, 2014, 148: 33–38
10 Müllegger S, Rashidi M, Fattinger M, et al. Surface-supported hydrocarbon π radicals show kondo behavior. J Phys Chem C, 2013, 117: 5718–5721
11 Peng Q M, Obolda A, Zhang M, et al. Organic light-emitting diodes using a neutral pi radical as emitter: The emission from a doublet. Angew Chem Int Ed, 2015, 54: 7091–7095
12 Obolda A, Ai X, Zhang M, et al. Up to 100% formation ratio of doublet exciton in deep-red organic light-emitting diodes based on neutral pi-radical. ACS Appl Mater Interfaces, 2016, 8: 35472–35478
13 PIotnikov V A S. The luminescence-spectroscopic properties of aromatic radicals and biradicals. Rus Chem Rev, 1986, 55: 929–947
14 López M, Velasco D, López-Calahorra F, et al. Light-emitting persistent radicals for efficient sensor devices of solvent polarity. Tetrahedron

Lett, 2008, 49: 5196–5199
15 Heckmann A, Dümmler S, Pauli J, et al. Highly fluorescent open-shell nir dyes: The time-dependence of back electron transfer in triarylamine-perchlorotriphenylmethyl radicals. J Phys Chem C, 2009, 113: 20958–20966
16 Lescop C, Luneau D, Bussière G, et al. Ligand-centered near-infrared luminescence from lanthanide complexes with chelating nitronyl nitroxide free radicals. Inorg Chem, 2000, 39: 3740–3741
17 Beaulac R, Bussière G, Reber C, et al. Solid-state absorption and luminescence spectroscopy of nitronyl nitroxide radicals. New J Chem, 2003, 27: 1200–1206
18 Beaulac R, Luneau D, Reber C. The emitting state of the imino nitroxide radical. Chem Phys Lett, 2005, 405: 153–158
19 Borozdina Y B, Kamm V, Laquai F, et al. Tuning the sensitivity of fluorophore-nitroxide radicals. J Mater Chem, 2012, 22: 13260–13267
20 Lussini V C, Blinco J P, Fairfull-Smith K E, et al. Polyaromatic profluorescent nitroxide probes with enhanced photostability. Chemistry, 2015, 21: 18258–18268
21 Beldjoudi Y, Osorio-Román I, Nascimento M A, et al. A fluorescent dithiadiazolyl radical: Structure and optical properties of phenanthrenyl dithiadiazolyl in solution and polymer composites. J Mater Chem C, 2017, 5: 2794–2799
22 Fox M A, Gaillard E, Chen C C. Photochemistry of stable free radicals: The photolysis of perchlorotriphenylmethyl radicals. J Am Chem Soc, 1987, 109: 7088–7094
23 Ruberu S R, Fox M A. Photochemical behavior of stable free radicals: The photochemistry of perchlorodiphenylmethyl radical. J Phys Chem, 1993, 97: 143–149
24 Ballester M, Riera J, Castañer J, et al. An easy, high-yield synthesis of highly chlorinated mono-, di- and triarylmethanes. Synthesis, 1986, 1986: 64–66
25 Armet O, Veciana J, Rovira C, et al. Inert carbon free radicals. 8. Polychlorotriphenylmethyl radicals: Synthesis, structure, and spin-density distribution. J Phys Chem, 1987, 91: 5608–5616
26 Gamero V, Velasco D, Latorre S, et al. [4-(n-carbazolyl)-2,6-dichlorophenyl]bis(2,4,6-trichlorophenyl)methyl radical an efficient red light-emitting paramagnetic molecule. Tetrahedron Lett, 2006, 47: 2305–2309

Summary for “咪唑取代的三苯甲基自由基的合成表征及其光学性质”

Synthesis and characterization of imidazole substituted trityl radicals and its optical properties

AI Xin & LI Feng*

State Key Laboratory of Supramolecular Structure and Materials, College of Chemistry, Jilin University, Changchun 130012, China
* Corresponding author, E-mail: lifeng01@jlu.edu.cn

Recently organic luminescent radical materials have attracted much attention as a class of novel luminescent materials which can produce doublet emission. Here we report two modified organic luminescent radicals TTM-Imz2 and TTM-Imz3 derived from tris(2,4,6-trichlorophenyl)methyl radical (TTM) through introduction of imidazole. Various measuring methods have been carried out to characterize the structure and radical properties of the two products, such as gas chromatography-mass spectrometer (GC-MS), Fourier transform infrared spectroscopy (FT-IR) and electron paramagnetic resonance spectrometer (EPR). The existence of single electron on two products has been confirmed by the EPR spectra with $g_{\text{TTM-Imz}_2}$=2.0040 and $g_{\text{TTM-Imz}_3}$=2.0038, which were close to the free electron (g=2.0023). Then, photo-physical properties have been characterized through ultraviolet-visible spectroscopy (UV-vis), steady state fluorescence spectroscopy, transient state fluorescence spectroscopy, and so on. Absorption spectra of TTM-Imz2 and TTM-Imz3 both have a strong absorption band at short wavelength and a week absorption band at long wavelength. For TTM-Imz2, its absorption peaks are λ=382 and 552 nm, and for TTM-Imz3, λ=390 and 558 nm. Emission spectra of TTM-Imz2 and TTM-Imz3 in various solvents do not show significant change. The emission peak of TTM-Imz2 is λ=581 nm in hexane, and for TTM-Imz3, λ=584 nm. Compared to the emission peak of TTM, they have bathochromic shift about 20 nm. Using rhodamine 6G in ethanol as a standard, the relative fluorescence quantum yields of TTM-Imz2 and TTM-Imz3 in chloroform have been determined under excitation with λ_{ex}=380 nm, which are up to 5.9% and 10.5% respectively. The excited luminescence lifetime (τ) of TTM-Imz2 and TTM-Imz3 in chloroform were 12.8 and 16.1 ns respectively determined by transient fluorescence decay. Furthermore, theoretical calculations have been carried out to study the molecular orbitals, electron distribution and the effect of imidazole moiety of the radicals. The DFT calculations (UB3LYP/6-31G(d, p)) results show that both of the radicals have propeller type planner structure with sp^2 hybridization central carbon atom. And the dihedral angle between imidazole moiety and its adjacent benzene ring is 33°–35°. The singly occupied molecular orbital (SOMO) is mainly distributed on the central carbon atom and partially delocalized onto the benzene rings and the imidazole rings. The energy gap between SOMO and the lowest unoccupied orbital of TTM-Imz2 and TTM-Imz3 are 2.22 and 2.19 eV, respectively, which are lower than that of TTM (2.32 eV). Thus, compared to TTM, both of the absorption peaks and the emission peaks of the products have bathochromic shift. Finally, TGA measurements were performed to test the thermostability of the radicals. The thermal-decomposing temperature of TTM-Imz2 and TTM-Imz3 are 129°C and 182°C respectively. Moreover, the fluorescence intensity decay of the radicals in toluene was recorded under excitation of a pulse laser with λ_{ex}=355 nm. The fluorescence intensity of TTM decreased rapidly with a half-time of 27.9 s, by contrast, TTM-Imz2 and TTM-Imz3 are more stable with a half-time of 1156.1 and 661.4 s, which are up to TTM’s 41.4 and 21.9 times. Finally, OLEDs of TTM-Imz2 and TTM-Imz3 have been fabricated. Both of the devices realized orange light emission. The maximum luminance of TTM-Imz3 reaches 147 cd/m^2, and the maximum EQE of TTM-Imz2 and TTM-Imz3 reaches 1.1% and 2.9% respectively. In conclusion, the introduction of imidazole moiety in TTM-Imz2 and TTM-Imz3 increase the fluorescence quantum yields and enhanced the stability of the TTM radicals effectively, and orange light emission has been realized both in solution and OLEDs.

organic luminescence radical, doublet, imidazole, orange light emission, fluorescence quantum yields, stability, OLEDs

doi: 10.1360/N972017-00896